A New Photosensitive Polymeric Material for WORM Optical Data Storage Using Multichannel Two-Photon Fluorescence Readout

Kevin D. Belfield* and Katherine J. Schafer

Department of Chemistry and School of Optics/CREOL, University of Central Florida, Orlando, Florida 32816-2366

Received September 18, 2001. Revised Manuscript Received June 19, 2002

We report image formation via photoinduced fluorescence changes in a polymeric medium with nondestructive two-photon fluorescence readout of a multilayer structure. A two-photon absorbing fluorescent dye possessing functional groups with differential basicity, (7-benzothiazolyl-9,9-didecyl-2,2-(*N*,*N*-diphenylamino)fluorene) (**1**), underwent protonation in the presence of a photoinduced acid generator upon exposure to a broadband UV light source or femtosecond near-IR laser irradiation. Solution studies demonstrated formation of monoprotonated and diprotonated species upon irradiation, each resulting in distinctly different absorption and fluorescence properties. The fluorescence of the original, neutral fluorophore was reduced upon monoprotonation, leading to a concomitant increase in fluorescence at longer wavelengths due to the monoprotonated form. Experiments in polymer films demonstrate the changes in fluorescence properties of the fluorophores can be employed for a write-once read-many (WORM) data storage medium with a two-photon fluorescence readout. Two-channel, two-photon fluorescence imaging provided both "positive" and "negative" image readout capability.

Introduction

Over the past 50 years, the field of organic photochemistry has produced a wealth of information, from reaction mechanisms to useful methodology for synthetic transformations. Many technological innovations have been realized during this time due to the exploits of this knowledge, including photoresists and lithography for the production of integrated circuits, photocharge generation for xerography, multidimensional fluorescence imaging, photodynamic therapy for cancer treatment, photoinitiated polymerization, and UV protection of plastics and humans through the development of UV absorbing compounds and sunscreens, to name a few. The scientific basis of many of these processes continues to be utilized today, particularly in the development of organic three-dimensional optical data storage media and processes.

With the ever-pressing demand for higher storage densities, researchers are pursuing a number of strategies to develop three-dimensional capabilities for optical data storage in organic-based systems. Among the various strategies reported are holographic data storage using photopolymerizable media,[1] photorefractive polymers,[2] and two-photon-induced photochromism,[3] to mention a few. It is known that fluorescence properties of certain molecules may be changed (quenched) upon protonation by photogeneration of acid.[4] We have reported two-photon-induced photoacid generation using onium salts and short pulsed near-IR lasers in the presence of a polymerizable medium, resulting in two-photon photoinitiated cationic polymerization.[5] The inherent three-dimensional features associated with two-photon absorption provides an intriguing basis upon which to combine spatially resolved, two-photon-induced photoacid generation and fluorescence quenching with nondestructive two-photon fluorescence imaging, eliminating the need for a fixing step.[5]

The quadratic, or nonlinear, dependence of two-photon absorption on the intensity of the incident light has substantial implications ($dw/dt \propto I^2$). For example, in a medium containing one-photon absorbing chromophores, significant absorption occurs all along the path of a focused beam of suitable wavelength light. This can lead to excitation outside the focal volume. In a two-photon process, negligible absorption occurs except in the immediate vicinity of the focal volume of a light beam of appropriate energy. This allows spatial resolution about the beam axis as well as radially, which circumvents out-of-focus absorption and is the principal reason for two-photon fluorescence imaging.[6] Particular molecules can undergo upconverted fluorescence through nonresonant two-photon absorption using near-IR ra-

* To whom correspondence should be addressed.

(1) See, for example, Cheben, P.; Calvo, M. *Appl. Phys. Lett.* **2001**, *78*, 1490.

(2) See, for example, Belfield, K. D.; Chinna, C.; Najjar, O.; Sriram, S.; Schafer, K. J. In *Field Responsive Polymers*; Khan, I. M., Harrison, J. S., Eds.; ACS Symposium Series 726; American Chemical Society: Washington, D.C., 1999; Chapter 17.

(3) Belfield, K. D.; Hagan, D. J.; Liu, Y.; Negres, R. A.; Fan, M.; Hernandez, F. E. In *Organic Photorefractives, Photoreceptors, and Nanocomposites, Proc. SPIE Vol. 4104*; Lewis, K. L., Meerholz, K., Eds.; SPIE-The International Society for Optical Engineering: Bellingham, WA, 2000; pp 15−22.

(4) Kim, J.-M.; Chang, T. E.; Kang, J.-H.; Park, K. H.; Han, D.-K.; Ahn, K.-D. *Angew. Chem., Int. Ed.* **2000**, *39*, 1780.

(5) Belfield, K. D.; Schafer, K. J.; Liu, Y.; Liu, J.; Ren X.; Van Stryland, E. W. *J. Phys. Org. Chem.* **2000**, *13*, 837.

(6) Denk, W.; Strickler, J. H.; Webb, W. W. *Science* **1990**, *248*, 73.

10.1021/cm010799t CCC: $22.00
Published on Web 08/02/2002

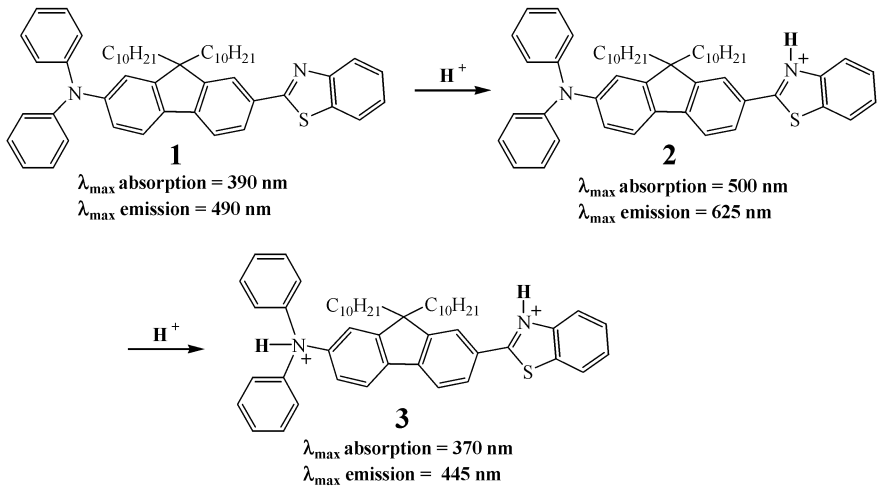

Figure 1. Reaction of fluorene **1** with acid, resulting in the formation of monoprotonated **2** and diprotonated **3** products.

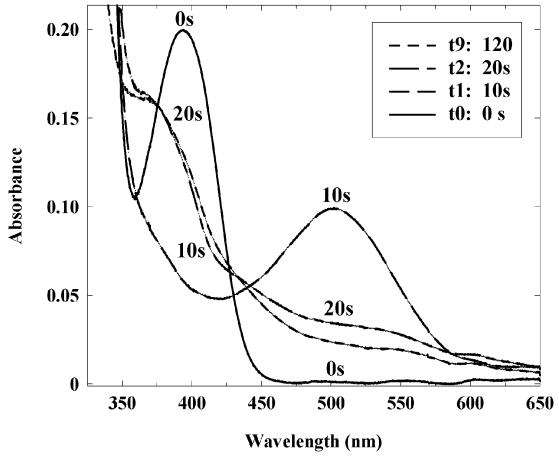

Figure 2. Time-dependent UV−visible absorption spectra of the irradiation of **1** and photoacid generator in CH_2Cl_2 at irradiation times from 0 to 120 s.

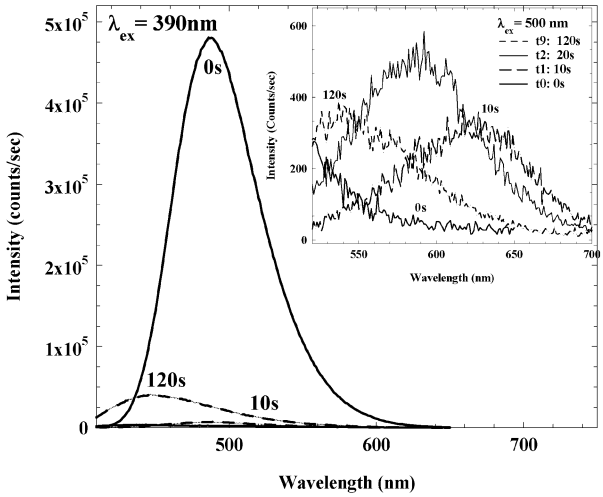

Figure 3. Time-dependent fluorescence emission spectra for the irradiation of **1** and photoacid generator in CH_2Cl_2 at irradiation times from 0 to 120 s (excitation at 390 nm). Inset shows fluorescence at longer wavelength with excitation at 500 nm.

diation, resulting in an energy emission greater than that of the individual photons involved.[7] The use of a longer wavelength excitation source for fluorescence emission affords advantages not feasible using conventional UV or visible fluorescence techniques, for example, deeper penetration of the excitation beam and reduction of photobleaching, and is particularly well-suited for fluorescence detection in multilayer coatings.

We previously reported the synthesis and characterization of organic fluorescent dyes with high two-photon absorptivity.[5,8,9] Several of these dyes also undergo substantial changes in the absorption and fluorescence spectral properties in the presence of strong acid, that is, they undergo protonation, affording changes in their polarizability, absorption and emission maxima, and fluorescence quantum yields.[10] We wish to report results of the photoinduced protonation of fluorene dye **1** in liquid solution and polymer thin films (Figure 1) and subsequent 3-D imaging of multilayer polymer films via two-photon fluorescence imaging, resulting in a write-once, read-many (WORM) optical data storage system.

Experimental Section

Materials. The photoacid generator, CD1010 (a triarylsulfonium hexafluoroantimonate salt as 50 wt % in propylene carbonate), was purchased from Sartomer and used as received. The synthesis and characterization of the two-photon absorbing fluorophore, 7-benzothiazoly-9,9-didecyl-2,2-(*N*,*N*-diphenylamino)fluorene (**1**), was described previously.[8] Polystyrene (PS) (molecular weight 35000) was purchased from Waters Associates and used directly. Phosphorylated poly(VBC-*co*-MMA) was prepared as previously reported, consisting of a mole ratio of diethyl vinylbenzylphosphonate to MMA of 1:3 in the polymer.[11] Acetonitrile (ACN), 1,4-dioxane, and CH_2Cl_2 (HPLC or spectrophotometric grades) were purchased from Sigma-Aldrich and were used as received. Various masks were used during the photoexposure of prepared polymer films, including TEM grids (400-mesh nickel square and 100-mesh

(7) Albota, M.; Beljonne, D.; Bredas, J.-L.; Ehrlich, J. E.; Fu, J.-Y.; Heikal, A. A.; Hess, S. E.; Kogej, T.; Levin, M. D.; Marder, S. R.; McCord-Moughon, D.; Perry, J. W.; Rockel, H.; Rumi, M.; Subramaniam, G.; Webb, W. W.; Wu, X.-L.; Xu, C. *Science* **1998**, *281*, 1653.

(8) Belfield, K. D.; Schafer, K. J.; Mourad, W. *J. Org. Chem.* **2000**, *65*, 4475.

(9) Belfield, K. D.; Schafer, K. J.; Hagan, D. J.; Van Stryland, E. W.; Negres, R. A. *Org. Lett.* **1999**, *1*, 1575.

(10) Belfield, K. D.; Bondar, M. V.; Przhonska, O. V.; Schafer K. J.; Mourad, W. *J. Lumin.* **2002**, *97*, 141.

(11) Belfield, K. D.; Wang, J. *J. Polym. Sci., Polym. Chem. Ed.* **1995**, *33*, 1235.

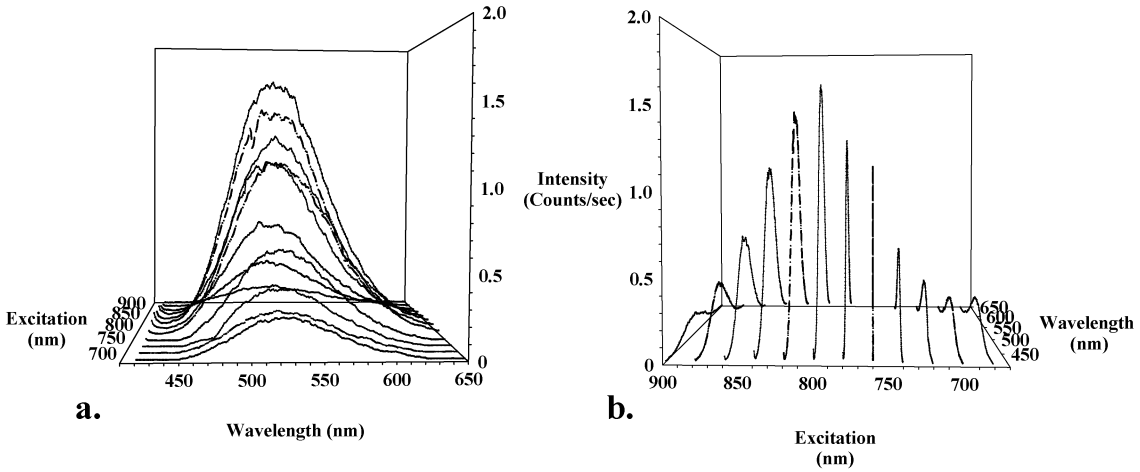

Figure 4. Two-photon upconverted fluorescence emission spectra of **1** at several femtosecond pulsed pump wavelengths (2.5×10^{-4} M, ACN).

hexagonal grids from Polysciences), glass resolution targets (negative slide with the 1951 USAF test pattern from Edmund Scientific), and photolithographic waveguide masks (from PPM Photomask, Inc).

Instrumentation. UV−visible absorption and fluorescence emission spectra from solutions were recorded with a Varian Cary 3 spectrophotometer and a Photon Technologies International (PTI) Quantamaster spectrofluorimeter fitted with one excitation monochromator (Xe lamp) and two emission monochromators (PMT detectors), respectively. Irradiation of solutions and thin films were performed in a Rayonet photoreactor containing broadband UV bulbs (300−400 nm). Polymer thin films were spin-coated onto either No. 1 glass microscope cover slips or 2.5 × 2.5 cm microscope glass slides (Fisher) with a spin-coater from Headway Research, Inc. The film thickness of polymer films was measured with a Tencor Instruments profilometer. The two-photon upconverted fluorescence emission spectra of the fluorophore were recorded with the PTI spectrofluorimeter using a Clark-MXR CPA-2001 laser system. Femtosecond (fs) pulses from a frequency-doubled erbium-doped fiber ring oscillator were stretched to about 200 ps, then passed through a Ti:Sapphire regenerative amplifier, and compressed down to 160 fs. The energy of the output single pulse (centered at $\lambda = 775$ nm) was 137 nJ at a 1-kHz repetition rate. This pumped a Quantronix OPO/OPA, producing femtosecond pulsed output, tunable from 550 nm to 1.6 μm. Two-photon fluorescence images of polymer films were performed on a modified Olympus Fluoview laser scanning confocal microscopy system equipped with a broadband, tunable Coherent Mira Ti:Sapphire laser (tuned to 800 nm, 115-fs pulse width, 76-MHz repetition rate), pumped by a 10-W Coherent Verdi frequency-doubled Nd:YAG laser, and a two-channel detection system (two Hamamatsu photomultiplier tubes with band-pass filters, channel 1: 510−550 nm, channel 2: 585−610 nm).

General Procedures. All solution studies were performed in CH_2Cl_2. Solutions were prepared containing 0.45 wt % polymer, 5.3×10^{-4} M PAG, and 5.8×10^{-5} M 7-benzothiazolyl-9,9-didecyl-2,2-(*N*,*N*-diphenylamino)fluorene (**1**). Solutions were transferred into a spectrofluorometer quartz cuvette cell fitted with a Teflon stopper and a small magnetic stir bar, which allowed for solution mixing during irradiation in the Rayonet photoreactor. All solvents and solutions were deaerated by bubbling with N_2 gas prior to spectroscopic measurements and were carefully protected from exposure to ambient or external light sources. Each solution was exposed for 120 s, with absorption and fluorescence emission spectra collected at 10-s intervals.

All polymer solutions (18 wt % polymer) were passed through a 0.45-μm glass filter, prior to spin-coating at a spin rate of 1500 rpm for 20 s. Films were dried under reduced pressure overnight and their thickness was measured by profilometry. Polymer film compositions were prepared from a mixture that typically contained 0.8 wt % of **1** (3 mg, 4×10^{-6} mol), 8 wt % of PAG (32 mg, 4×10^{-5} mol), and 362 mg of polymer. The dried films were then exposed to UV light for various durations through a mask and, following mask removal, two-photon fluorescence imaging was performed on single and mutilayered films.

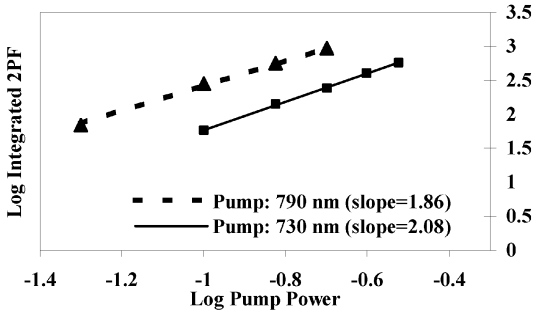

Figure 5. Plot of the total integrated fluorescence intensity of **1** as a function of pump power at 2-fs pump wavelengths.

Results and Discussion

Fluorene **1** was previously shown to undergo two-photon absorption and upconverted fluorescence on exposure to near-IR femtosecond laser irradiation.[5,8] The two-photon absorbing dye **1** contains basic nitrogen-containing benzothiazolyl and triarylamino groups that are sensitive to the presence of acids. Pohlers et al. have demonstrated the absorption spectrum of an acid-sensitive dye containing the benzothiazole group red shifts upon protonation in the presence of a photoacid generator (PAG).[12] Due to differences in basicity (pK_b), fluorene **1** undergoes selective, stepwise protonation, first by protonation of the benzothiazolyl nitrogen ($pK_b \cong 13$)[13] and then the triarylamino nitrogen ($pK_b \cong 19$).[14] This leads to a mixture of three species in Figure 1 (**1**, **2**, and **3**), each with distinct UV−visible absorption and fluorescence emission properties.

To understand the behavior of the two-photon absorbing fluorophore and predict results expected in solid thin

(12) Pohlers, G.; Scaiano, J. C.; Sinta, R. *Chem. Mater.* **1997**, *9*, 3222.
(13) Dey, J. K.; Dogra, S. K. *Bull. Chem. Soc. Jpn.* **1991**, *64*, 3142.
(14) Arnett. E. M.; Quirk, R. P.; Burke, J. J. *J. Am. Chem. Soc.* **1970**, *92*, 1260.

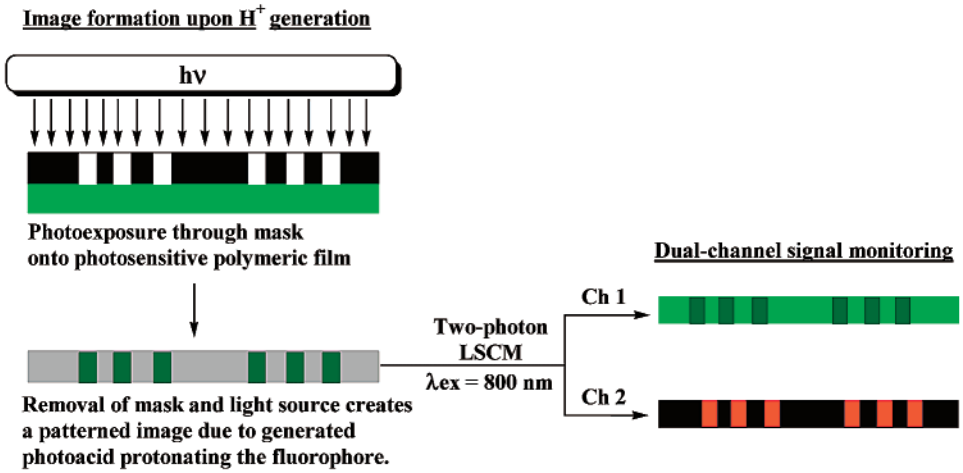

Figure 6. Diagram of image formation within a photosensitive polymeric film containing PAG, and acid-sensitive fluorophore, allowing two-photon-induced, dual-channel fluorescence imaging.

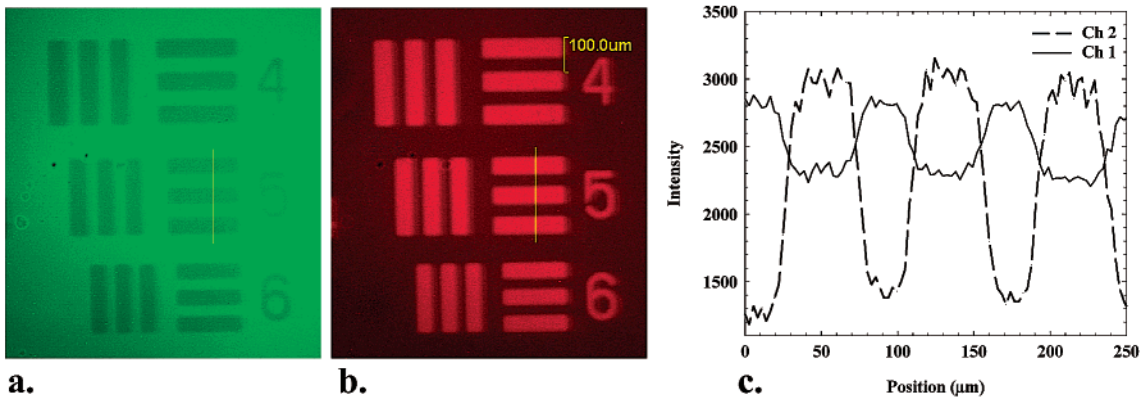

Figure 7. Two-photon fluorescent images of photosensitive films developed (via 350-nm broadband exposure, 4.4 mW/cm^2) using an Air Force resolution target mask. (a) Image recorded by channel 1, (b) image recorded by channel 2, and (c) fluorescence intensity by scanning an *xy* line across one set of three-membered elements (yellow line across set 5).

film studies, solution studies were performed in CH_2Cl_2. Time-dependent UV−visible absorption spectra for a solution containing **1** and the photoacid generator CD1010 (a triarylsulfonium salt) illustrate this nicely, as shown in Figure 2. Upon irradiation with broadband UV light (300−400 nm, 0.57 mW/cm^2), **1** undergoes protonation, resulting in the formation of **2** whose absorption spectrum is red-shifted by about 100 nm relative to that of **1**. The conversion of the neutral fluorophore **1** at early irradiation times (10 s) results in decreasing absorbance at its maximum at 390 nm and increasing absorbance at 500 nm upon generation of the protonated form, **2**. The red shift was expected since fluorene **1** is of an electron donor-π-acceptor construct and protonation of the benzothiazolyl acceptor increases the electron deficiency of this group, affording a greater dipole moment and polarizability. When **2** undergoes protonation, a new absorption that is blue-shifted relative to both **1** and **2** was observed due to the fact that the once electron-donating diphenylamino group in **1** and **2** has been converted to an electron-accepting moiety (quaternary ammonium salt) in **3**. The absorption due to the triarylsulfonium salt (λ_{max} = 310 nm) also decreases with time as expected but, for clarity, is not displayed in Figure 2. No evidence for charge-transfer complex formation was observed between fluorene **1** and the PAG; however, more detailed investigations would be needed to fully explore this possibility.

Changes in the fluorescence emission spectra corresponded with the observed changes in the absorption spectra. Protonation of **1** also resulted in a reduction of its fluorescence emission, while emission at longer wavelengths was observed due to excitation of the longer wavelength absorbing monoprotonated **2** (Figure 3). As can be seen, the fluorescence emission intensity at ca. 490 nm (390 nm excitation wavelength) decreases with irradiation while, at early exposure times, emission at ca. 625 nm appears, which then blue shifts upon further protonation to **3**. The emission at 625 nm is from monoprotonated **2** upon excitation at 500 nm. Eventually, diprotonation results in a relatively weak, blue-shifted emission at ca. 445 nm (from **3**). Thus, in addition to observing fluorescence quenching at ca. 490 nm, fluorescence enhancement (creation) at longer wavelengths (ca. 625 nm) is observed upon short irradiation times. As demonstrated in the following section, this behavior facilitates two-channel fluorescence imaging, resulting in contrast due to fluorescence quenching at the shorter wavelengths ($\lambda_{emission}$ of **1** from 425 to 620 nm) and fluorescence enhancement at longer wavelengths ($\lambda_{emission}$ of **2** from 520 to 700 nm).

To demonstrate the ability of fluorene **1** to exhibit two-photon upconverted fluorescence emission, fluores-

cence spectra were recorded upon excitation at a number of wavelengths using femtosecond near-IR excitation. Two-photon upconverted fluorescence spectra (2.5×10^{-4} M, ACN) pumped with femtosecond pulsed, near-IR are illustrated in Figure 4a,b. The neutral fluorophore **1** displayed upconverted fluorescence emission over a wide pump range, from 680 to 880 nm (Figure 4a) while, from Figure 4b, it is readily apparent that maximum two-photon upconverted fluoresence intensity was observed when pumped at 800 nm. To further confirm that **1** underwent two-photon absorption, the total integrated fluorescence intensity was determined as a function of incident intensity (pump power). Fluorescence from a two-photon absorption process will exhibit a quadratic dependence on incident intensity. Indeed, Figure 5 confirms that fluorene **1** underwent two-photon absorption as evidenced by the quadratic relationship between fluorescence emission intensity at several pump powers at two different pump wavelengths.

Next, thin polymer films (ca. 2−3-μm film thickness) were prepared by spin coating (on glass) a mixture of fluorene **1**, the photoacid generator, and polystyrene or, alternatively, phosphorylated poly(VBC-*co*-MMA) in a 1:3 v/v solution of acetonitrile/dioxane.[15] The phosphorylated copolymer was chosen due to its excellent solubility, ability of the polymer to solubilize organic dyes, and particularly the triarylsulfonium salt, without phase separation, and our extensive experience using this in thin film applications. A mixture of dry 1,4-dioxane/CH_3CN was found to be a good solvent for both spin coating and solution casting films of this polymer. Additionally, the polymer, PAG, and fluorophore were readily soluble in this mixture. Films were examined by optical microscopy for phase separation, with none observed, even at PAG concentrations over 10 wt %. Films were exposed to UV light through a number of different masks, including TEM grids, Air Force resolution targets, and photolithographic waveguide masks (Figure 6). After mask removal, two-photon fluorescence image collection was performed on the exposed films in single layers or multilayers.

Results analogous to those obtained in solution studies were observed but, quite fortuitously, the slower acid generation/protonation rate resulted in the formation and stabilization of monoprotonated fluorene **2**. With the beam focused in the plane of the fluorophore-containing layer, fluorescence intensity was recorded with both channel 1 (green) and channel 2 (red) simultaneously. The contrast in the "green" channel was due to the decrease in fluorescence of fluorene **1** (whose concentration decreases with irradiation). Contrast in the "red" channel was due to the fluorescence of monoprotonated **2** (whose concentration increases with irradiation).

Parts a and b of Figure 7 show films exposed using an Air Force image resolution target with images recorded by both channels. The large differences in fluorescence intensity in exposed and unexposed regions as well as the reverse parity of the images in the two channels, i.e., "positive" and "negative" image formation

(15) Photosensitive polymer film compositions typically contained 0.8 wt % (4×10^{-6} mol) of fluorene **1** and 8 wt % (4×10^{-5} mol) of CD1010 relative to the polymer.

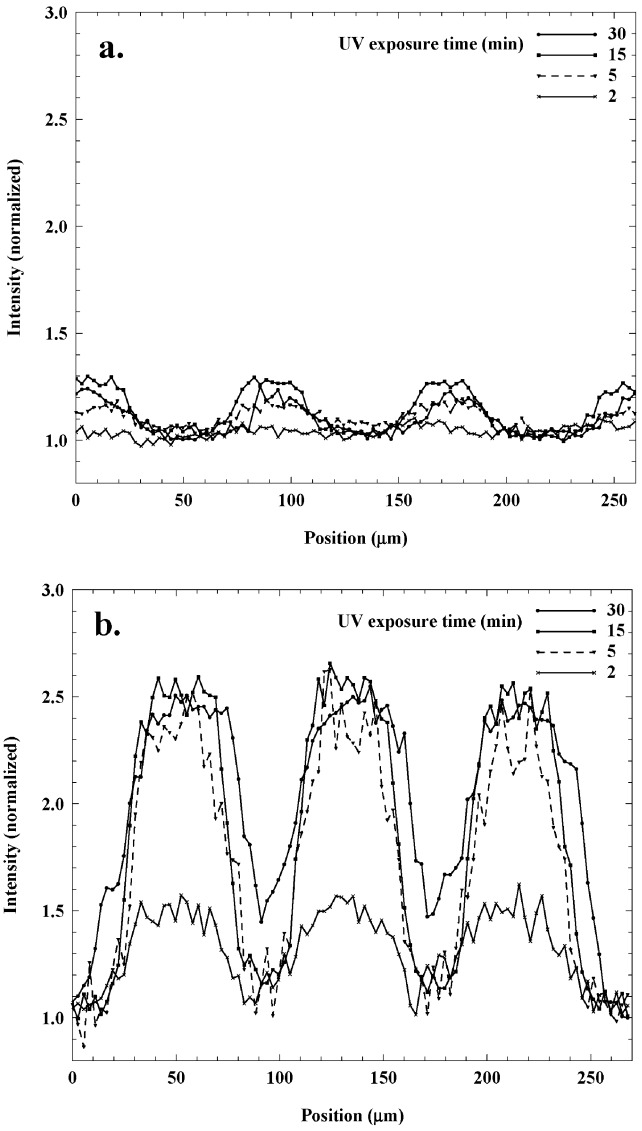

Figure 8. Fluorescence intensity plots versus position (*xy* line across a three-membered element) as a function of exposure time. (a) Intensity monitoring with channel 1 (fluorescence decreases in exposed areas over time) and (b) intensity monitoring with channel 2 (fluorescence enhancement in exposed areas over time) clearly shows the reverse parity of the signals.

from one system, can be clearly seen in the graph (Figure 7c) . Time-dependent studies were performed by irradiating the films for various times to determine the optimal contrast for each detection channel. The fluorescence intensity profiles as a function of exposure time and position across one set of the elements for each image is shown in parts a and b of Figure 8. Optimal exposure time can be established by identifying the intensity profile that would provide the best signal-to-noise ratio, minimizing the hazard of overexposing films that may compromise resolution due to acid diffusion.

For demonstrative purposes, multilayer assemblies were constructed by placing an uncoated glass cover slip between two cover slips coated with patterned photosensitive films, with the coated sides against the middle cover slip (Figure 9). Three-dimensional two-photon fluorescence imaging was performed on the multilayer structures.

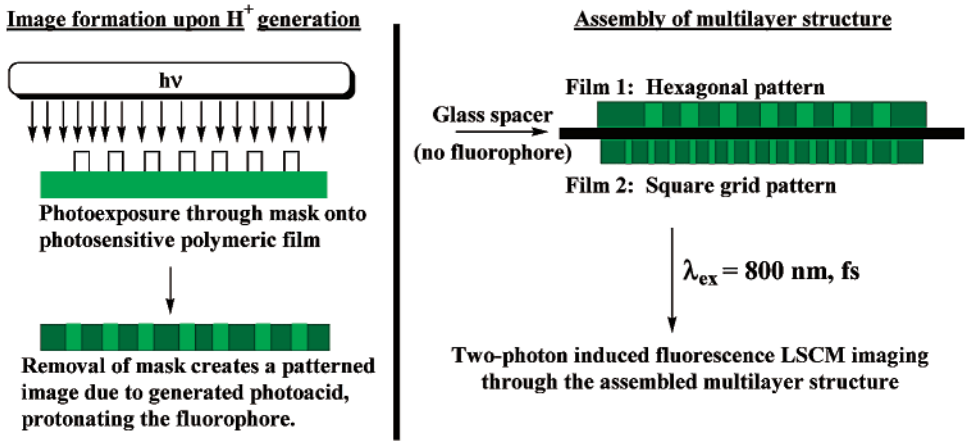

Figure 9. Image formation (upon photoacid generation) within photosensitive polymer films for assembly of multilayered structures. Two-photon fluorescence LSCM imaging using femtosecond pulsed near-IR pump allows for 3-D volumetric imaging of the layered structure.

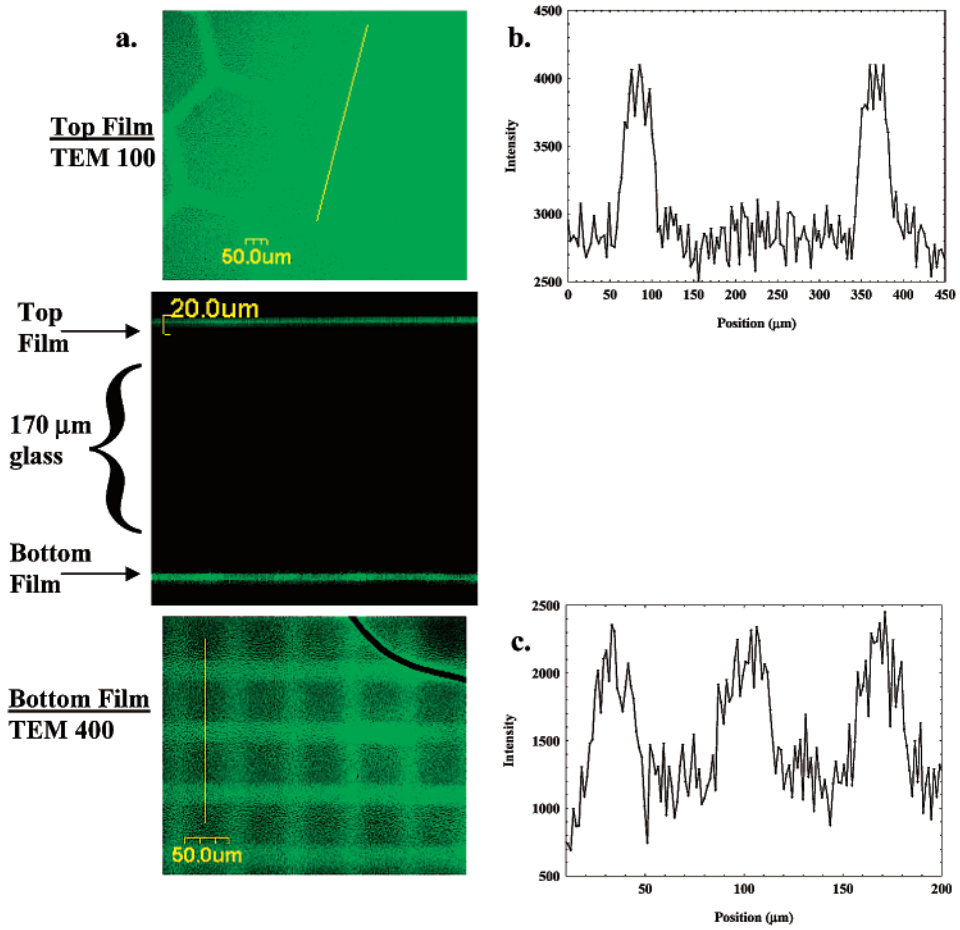

Figure 10. (a) Two-photon fluorescent images of multilayered films developed via 350-nm broadband irradiation (6.0 mW/cm^2) by exposure through TEM hexagonal and square grid masks. Fluorescence intensity plots for a line scan across a region (as defined by the yellow line across the image area) provides (b) image readout in one layer and (c) changing the depth (*z* position) for image (signal) readout in the lower layer within a multilayered system.

Two-photon fluorescent images of the photosensitive films constructed in a multilayer configuration (developed via UV exposure through TEM square and hexagonal grid masks) are displayed in Figure 10a. An *xy* planar scan of each film (hexagonal grid image on the top and square grid image on the bottom) within the multilayer, by focusing and scanning within the plane of the films, clearly shows the photopatterned image resulting from formation of the protonated species in exposed areas. A cross-sectional scan, where an *xy* line scan is stepped in the *z* dimension (multilayered image between the grid images in Figure 10a), clearly displays the separate film layers and demonstrates the three-dimensional nature of image formation possible within layered assemblies and the nondestructive optimal sectioning ability of two-photon fluorescent imaging. The signal readout (Figure 10b,c) establishes the possibility for a WORM binary optical data storage me-

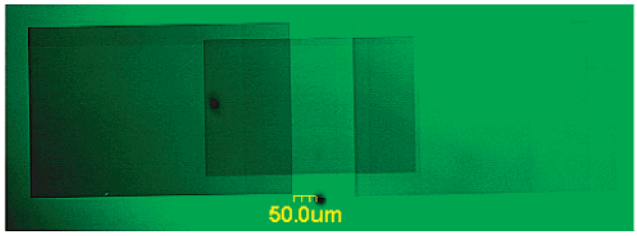

Figure 11. Image written (740 nm) and read (800 nm) in a photosensitive polymer film (1.5 μm) via two-photon excitation.

dium, where the valleys can be designated as a "0" and the peaks a "1".

Finally, both writing and recording were accomplished by two-photon excitation of a fluorophore/PAG photosensitive polymer film in which writing was accomplished by *xy* scans at 740 nm (115 fs, 76 MHz). The written image was read by a two-photon fluorescence imaging at 800 nm (115 fs, 76 MHz), as shown in Figure 11. Thus, image writing and reading has been accomplished via near-IR two-photon excitation of polymer films containing fluorophore **1** and a photoacid generator. The behavior and relative stability of **1** makes this compound a good candidate for WORM three-dimensional memory systems with writing and reading accomplished via two-photon fluorescence imaging.

Acknowledgment. The National Science Foundation (ECS-9970078, DMR9975773), the Research Corporation, and the donors of the Petroleum Research Fund of the American Chemical Society are gratefully acknowledged for support of this work. Profs. Eric W. Van Stryland and David J. Hagan are acknowledged for providing assistance.

CM010799T